Journal of Power Sources 237 (2013) 41–46

Contents lists available at SciVerse ScienceDirect

Journal of Power Sources

journal homepage: www.elsevier.com/locate/jpowsour

Free-standing graphene–carbon nanotube hybrid papers used as current collector and binder free anodes for lithium ion batteries

Yuhai Hu, Xifei Li, Jiajun Wang, Ruying Li, Xueliang Sun*

Department of Mechanics and Materials Engineering, The University of Western Ontario, London, ON, Canada N6A 5B9

HIGHLIGHTS

- ► Highly free-standing CNT-graphene papers with controlled CNT/graphene ratios were fabricated.
- ► The lithium ion storage capacities are strongly dependent on CNT/graphene ratios.
- ► The CNT-graphene papers exhibited high lithium storage capacities.
- ► The intrinsic factors that mediate the electrochemical performances were articulated.

ARTICLE INFO

Article history:
Received 27 October 2012
Received in revised form
4 January 2013
Accepted 22 February 2013
Available online 7 March 2013

Keywords:
Graphene
Graphene paper
Free standing
Anode
Lithium ion battery
Electrochemical energy storage

ABSTRACT

Free-standing hybrid papers were fabricated by the vacuum-assisted filtration of graphene nanosheets (GNS) and carbon nanotubes (CNTs) both suspended in water, an approach that is environmentally benign. The CNTs are randomly dispersed between the GNS and hence, the hybrid papers exhibit high mechanical strength and flexibility even after being annealed at 800 °C. Electrochemical properties of the hybrid papers are strongly dependent on the CNT/GN ratios. Highest lithium ion storage capacities were obtained in the paper with a CNT/GN ratio of 2:1. The initial reversible specific capacities are ~375 mAh g^{-1} at 100 mA g^{-1}. The capacities remain above 330 mAh g^{-1} after 100 cycles, which are about 100 mAh g^{-1} higher than those of the graphene paper with nearly the same mass. The improved capacities were attributed to the contribution of the CNTs, which prevent restacking of the GNS, increase cross-plane electric conductivity of the paper and simultaneously, store Li ions. These results suggest that graphene–CNT hybrid paper has a high potential to be used as collector and binder free anodes for lithium ion batteries.

1. Introduction

Huge market demand for zero-emission electric vehicles is a major drive for research and development of high energy-capacity rechargeable lithium ion batteries (LIBs). Carbon is one of the important and traditional anode materials for LIBs. Although graphite only possesses a theoretical capacity of ~372 mAh g^{-1}, delicate assembly and fabrication offers carbons with novel morphologies that deliver capacities obviously higher than this value [1,2]. Graphene, a single layer of graphite, can offer a theoretical capacity over 700 mAh g^{-1}, and has been extensively investigated either directly as anodes or as electric conductor/mattress (forming composites) [3–8]. Moreover, as a result of their two-dimension structure, graphene nanosheets (GNS) can build up novel macroscopic structures, e.g., thin films and papers, opening new windows for graphene applications [9]. When used in LIBs, this type of assembly brings several evident advantages over traditional procedure for anode fabrication. The binder (an insulator) and the current collector (usually copper foil) are not needed, improving the specific capacity of a "whole" LIB. The graphene papers are also mechanically strong and flexible and therefore, could be used in thin film battery fabrication.

However, the existing data have manifested that the specific capacities of graphene papers are much lower than those of graphene powders due to the barrier for Li diffusion resulting from close stacking of the GNS in the papers [10–12]. This prevents the practical applications of graphene papers in LIBs. As such, many approaches have been proposed to improve the Li storage capacities of graphene-based papers [13–17]. Whereas high capacities (over 1000 mAh g^{-1}) were achieved, these approaches inevitably diminish the mechanical strength of the papers. To date, it still remains a significant challenge to improve the specific capacities of

* Corresponding author. Tel.: +1 519 661 2111x87759.
E-mail addresses: xsun9@uwo.ca, xsun@eng.uwo.ca (X. Sun).

0378-7753/$ – see front matter © 2013 Elsevier B.V. All rights reserved.
http://dx.doi.org/10.1016/j.jpowsour.2013.02.065

graphene papers and simultaneously, preserve their mechanical strength and flexibility.

Along these lines, we are focused on fabricating graphene-based hybrid papers that exhibit higher specific capacities than and mechanical strength comparable to those of graphene papers. For this, we take an aim at methods that are cost efficient, environmentally benign and easy to be scaled up. Carbon nanotubes (CNTs) are adopted because of their one-dimensional structure and high electric conductivity. CNTs have a longer history than graphene does, and there are a great number of studies attempting to incorporate CNTs into electrode materials for LIBs either directly as an anode or as a conductive dopant [18–23]. Among them, CNT papers (free standing or CNTs aligned onto a conductive substrate by chemical vapor deposition (CVD) method), receive increasing interest rapidly [24–26]. Nevertheless, such assemblies of CNTs are usually with lower mechanical strength and more importantly, the yield is low and the practical application is yet seen. Recently, there are also several studies on fabrication of GN–CNT nanocomposites [27,28], but the free-standing papers were never reported.

In this paper, free-standing GN–CNT hybrid papers were fabricated by the vacuum-assisted filtration of GNS and CNTs both suspended in water. The CNTs are randomly dispersed between the GNS (with GNS predominating) and hence, high mechanical strength and flexibility are preserved for the papers. In such an assembly, the presence of CNTs is expected to play multiple roles including (1) prevent restacking of GNS during the process of paper fabrication, allowing more effective contact between the electrolyte (Li) and the GNS in the interior of the paper, (2) increase cross-plane conductivity of the paper as CNTs also have high electric conductivity and can closely contact with GNS, and (3) store Li. Battery performances of the hybrid papers are highly dependent on the CNT/GN ratios. Highest capacities were obtained in the paper with a CNT/GN volume ratio of 2:1, which exhibited initial reversible specific capacity of ~375 mAh g^{-1} (2nd cycle) and 330 mAh g^{-1} at the 100th cycle.

2. Experimental

2.1. Fabrication of GNS and CNT dispersion

Graphene oxide was synthesized using a modified Hummers method [29]. Typically, graphite was oxidized with $KMnO_4$, $NaNO_3$, and H_2SO_4. As synthesized graphite oxide was dispersed in deionized (DI) water to give rise to a 0.5 mg ml^{-1} dispersion, and was then exfoliated by ultrasonication for 1 h. The obtained dispersion was centrifuged at 5000 rpm for 15 min to obtain a homogeneous graphene oxide dispersion. Commercial CNTs from Shenzhen Nanotech Port Co., Ltd. were used as-received without further purification. 100 mg CNTs were dispersed with Triton X-100 (100 mg) as a surfactant in 100 mL DI water to form a dispersion through ultrasonication. The obtained dispersion was purified by centrifuge treatment to remove impurities and tangled CNTs.

For fabrication of GN–CNT hybrid papers, requisite amounts of the GNS and CNTs, both suspended in water, were mixed by ultrasonication for 0.5 h. The mixtures were then filtrated under the assistance of vacuum through an Anodisc membrane filter (47 mm diameter, 0.2 μm pore size; Whatman), followed by air drying for 24 h at room temperature and peeling from the filter. The whole process is shown in Fig. 1. Before spectroscopic and electrochemical characterization, the graphene papers were mildly annealed in Ar-H_2 (10% H_2) atmosphere at 800 °C for 2 h for additional deoxygenation. For simplicity, the hybrid papers were denoted as *x*CNT–*y*GN. For example, 20CNT–20GN is corresponding to a paper with 20 mL CNTs and 20 mL GNS dispersions.

2.2. Characterization

Morphologies of the papers were checked using a field emission scanning electron microscope (Hitachi S-4800). Raman spectra were obtained using a HORIBA Scientific LabRAM HR Raman spectrometer system equipped with a 532.4 nm laser as the exciting radiation. The system is also equipped with an optical microscope so as to give rise to confocal signals. To obtain charge–discharge profiles and cycle performance data, the papers were used as anode directly and were assembled in a CR 2032-type coin cell configuration, i.e., no binder and current collector are involved. A lithium foil was used as a counter electrode. Electrolyte was composed of 1 M $LiPF_6$ salt dissolved in a solution consisting ethylene carbonate, diethyl carbonate, ethyl methyl carbonate (1:1:1 in volume). Assembly of the batteries was fully carried out in an Ar-filled glove box with oxygen and water levels <1 ppm. Charge–discharge characteristics were tested galvanostatically in a voltage range of 0.01–3.0 V (vs. Li^+/Li) at a desired current density using an Arbin BT-2000 Battery Test System. Cyclic voltammetry (CV) tests were performed on a versatile multichannel potentiostat 3/*Z* (VMP3) at a scan rate of 0.1 mV s^{-1} over a potential range of 0.01–3.0 V (vs. Li^+/Li).

3. Result and discussion

3.1. Characterization of the hybrid papers

Several hybrid papers were fabricated through a same procedure, including 6.5CNT–20GN (0.39 mg), 20CNT–20GN (0.27 mg)

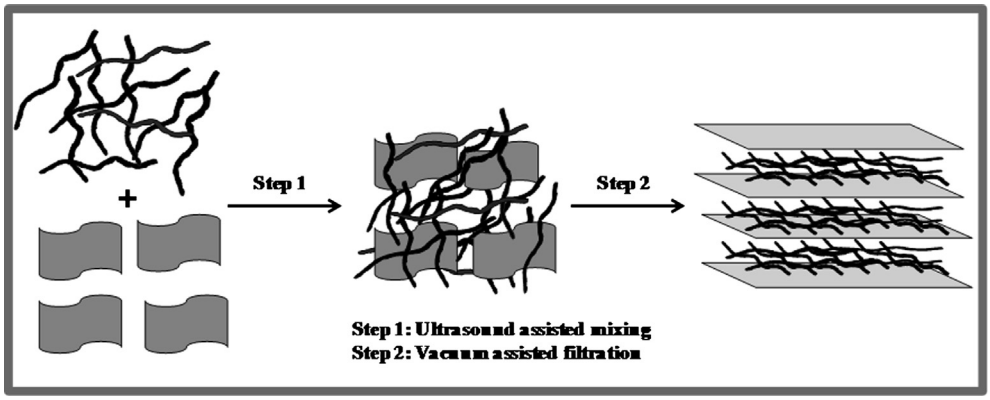

Fig. 1. Schematic diagram of fabrication of the CNT–GN papers by vacuum-assisted filtration.

and 20CNT–10GN (0.13 mg), respectively. For the 20 GN papers, the decline in the mass following the increase in the CNT loading is assumed to result from the filtering process. The GNS in the suspension have different sizes, and some are smaller than 200 nm. When more CNTs are present in the mixed suspension, e.g., the 20CNT–20GN, the CNTs, due to their one-dimension structure, retard the formation of a dense thin film of graphene on the filter and hence, more CNTs and smaller-size GNS pass through the filter and are dumped. Notice the pore size of the filter is 220 nm.

All the hybrid papers possess high mechanical strength and flexibility, which are similar to that of the graphene paper, as shown in Fig. S1. Surface morphologies of the 6.5CNT–20GN and 20CNT–10GN papers are shown in Fig. 2(a) and (b) as examples. Obviously, for both papers, the CNTs are wrapped with the GNS, and the paper surface is mainly composed of the GNS. More CNTs are observed in the 20CNT–10GN image. The 20CNT–10GN image also has a much higher resolution than the 6.5CNT–20GN image does (several papers were checked and compared), suggesting that the electric conductivity of the 20CNT–10GN paper is higher. Obviously, the enhanced electric conductivity results from the CNTs. In the graphene papers, the distance between the GNS (~0.379 nm) is larger than that in graphite (~0.336 nm) [10], meaning that electric conductivity in the cross-plane direction (perpendicular to the paper surface) is relatively lower. The CNTs, which are highly conductive and are able to closely contact with the GNS due to their strong $\pi-\pi$ interactions [23,27], work as a bridge between the GNS that allows the cross-plane electron flow feasible, hence improving the electric conductivity of the paper. Such an assembly of the GNS and the CNTs is more clearly manifested by the cross-section images of the papers, as shown in Fig. 2(c) and (d). Here, the 20CNT–20GN paper was characterized instead of the 6.5CNT–20GN paper because of its relatively higher CNT content. Interestingly, (1) the CNTs are randomly dispersed between the GNS and are aligned with their axials parallel to the paper surface; (2) there are more CNTs in the 20CNT–10GN paper; (3) the CNTs indeed closely contact with GNS; and (4) the 20CNT–20GN paper is relatively thicker, i.e., 1.2 μm vs. 0.8 μm. It is worth mentioning that the white spots in the 20CNT–10GN images are corresponding to carbon particles that are generated during thermal treatment of the papers. A similar phenomenon was also observed in our NH_3-treated graphene papers, for which NH_3-induced chemical etching gives rise to pores and carbon particles (see Fig. S2). Our other experiments prove that they do not affect battery performance of the papers at all.

Raman spectra of the papers are shown in Fig. 3. There are no discernable changes in the spectra following the increase in the CNT/GN ratios as long as the ratios are ≤1 (20:20). Only the two peaks corresponding to the D-band (1342 cm^{-1}) and the G-band (1580 cm^{-1}) of the GNS are detected. Their relative intensities remain almost constant, i.e., $I_D/I_G \cong 1.1$. Spectral change happened to the 20CNT–10GN paper. The D-band loses intensity evidently, and the I_D/I_G declines to 0.85. This is a typical feature of CNTs as there are less defect sites in them [30,31]. These results corroborate those of SEM, i.e., there are more CNTs in the 20CNT–10GN paper, and the CNTs are mostly wrapped with the GNS.

3.2. Electrochemical characterization of the hybrid papers

The interactions between Li and the papers (intercalation and de-intercalation) were first characterized using a cyclevoltammetry (CV) method. The characterization employed the hybrid paper as electrodes in 1.0 M $LiPF_6$ electrolyte and with lithium sheet as the counter and reference electrodes. CV curves of the 6.5CNT–20GN and the 20CNT–10GN papers are shown in Fig. 4. There is no big difference between the two types of curves. During the first discharge (intercalation of Li), a peak appears at ~0.69 V and ~0.59 V in the 20CNT–10GN curve and the 6.5CNT–20GN curve, respectively. Both peaks are corresponding to the solid electrolyte interphase (SEI) formation on the anode surface [32]. Such peaks are not detected in the following cycles. The peak close

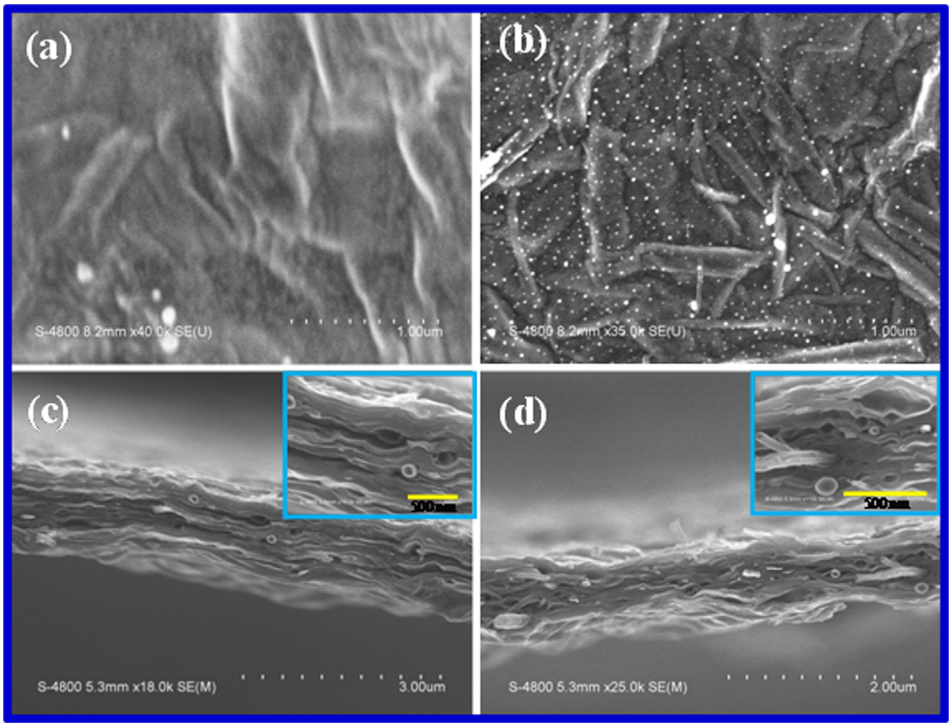

Fig. 2. SEM images of the CNT–GN papers: (a) and (b) top views of the 6.5CNT–20GN and 20CNT–10GN papers, respectively; (c) and (d) cross-sections of the 20CNT–20GN and 20CNT–10GN papers, respectively.

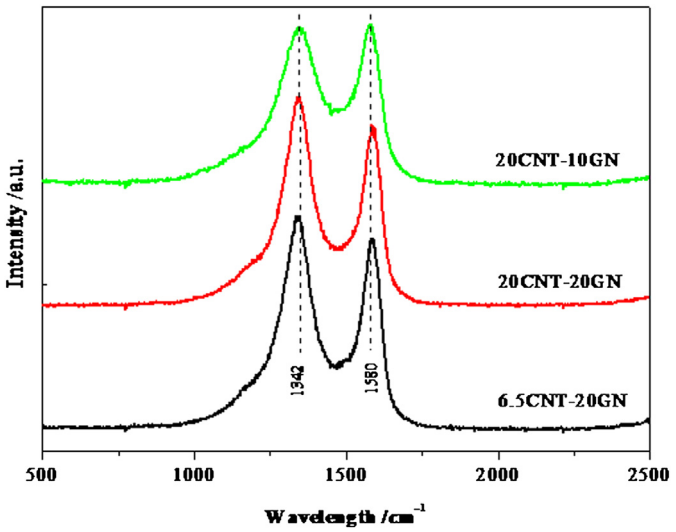

Fig. 3. Raman spectra of the CNT–GN papers.

to 0 V corresponds to lithium intercalation into the GNS and the CNTs, a typical feature of Li–carbon interaction [33]. Nevertheless, it is worth noting that a peak at ~0.17 V appears in the 20CNT–10GN curve but not in the 6.5CNT–20GN curve. This peak remains a weak intensity in the second and third cycles, and can be ascribed to lithium intercalation into the graphene layers like the disordered carbon material due to the structural defects in some basal planes of carbon nanosheets in the graphene paper [10,33]. Obviously, the presence of CNTs brings more defects into the paper.

Battery performances of the hybrid papers were tested at 100 mA g^{-1} and are shown in Fig. 5. The specific capacities of the CNTs (with the powder based CNTs pasted on a copper current collector) are only between 200 and 160 mAh g^{-1} in the first 100 cycles, as shown in Fig. S3. A 0.15 mg graphene paper (without CNTs), which was fabricated by assembly of graphene oxide nanosheets followed by an annealing at 800 °C, exhibits the reversible specific capacities >250 mAh g^{-1} in the first 50 cycles. The capacities of the 6.5CNT–20GN hybrid paper are considerably lower than those of the graphene paper, e.g., the reversible specific capacities are between 180 and 150 mAh g^{-1} in the 50 cycles. At higher CNT/GN ratios, higher capacities are gained, i.e., in the first 50 cycles, the capacities were kept at ~250 mAh g^{-1} for the 20CNT–20GN paper and >330 mAh g^{-1} for the 20CNT–10GN paper, respectively. The >330 mAh g^{-1} capacities are very close to the theoretical capacity of graphite, i.e., 372 mAh g^{-1}.

Considering that battery performance of graphene paper is strongly dependent on paper thickness, we further compared the performances of the graphene paper (0.15 mg) and the 20CNT–10GN paper (0.13 mg). As shown in the inserted panel, the capacities of the hybrid paper are ~100 mAh g^{-1} higher. Obviously, it is reasonable to conclude that the CNT–GN hybrid paper has higher battery performances than graphene paper does when the loadings of CNT and GN are properly adjusted, and the presence of CNTs plays a major role.

3.3. Characterization of the tested papers

The papers still preserve high strength and flexibility after cycles. SEM images of the tested 20CNT–20GN and 20CNT–10GN papers are shown in Fig. 6. Big changes are observed on the surfaces of both papers, and the changes are also obviously related to the CNT/GN ratios. The 20CNT–20GN surface is covered with tiny particles and some CNTs. The particles are also found on the surface

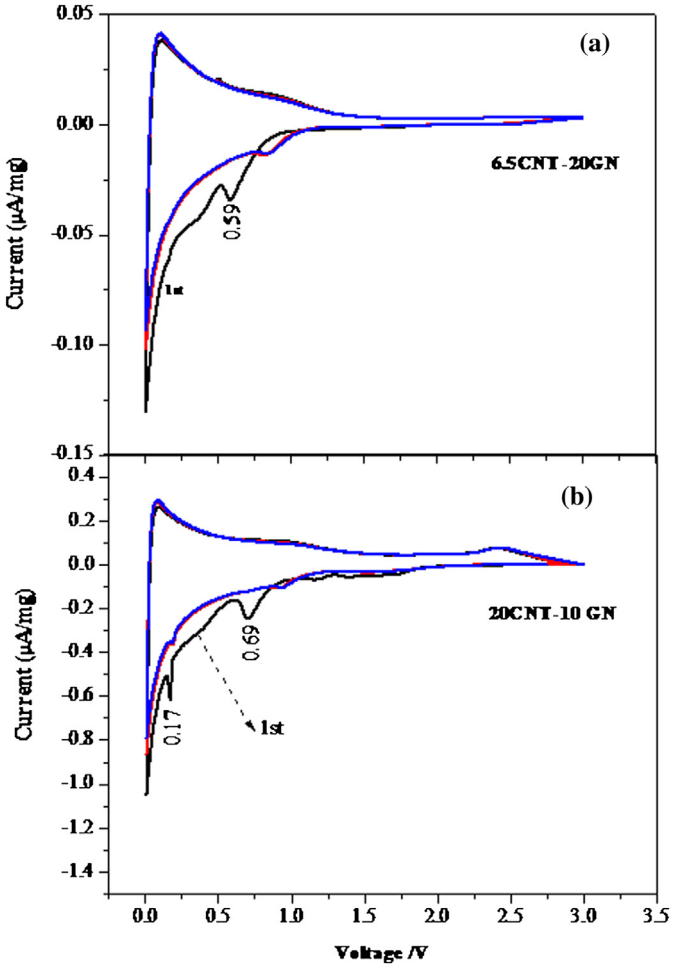

Fig. 4. Cyclic voltammetry curves of the 6.5CNT–20GN (a) and the 20CNT–10GN (b) papers.

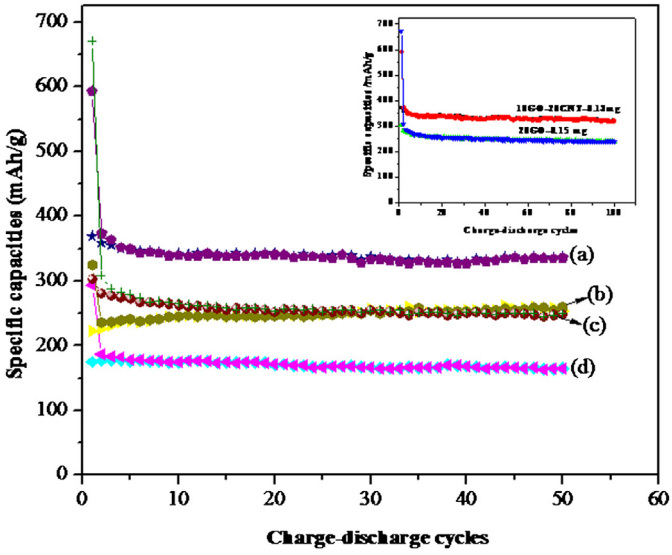

Fig. 5. Electrochemical characterization of the CNT–GN papers as anode tested at a current rate of 100 mA g^{-1}: (a) 20CNT–10GN; (b) 20CNT–20GN; (c) graphene paper; (d) 6.5CNT–10GN.

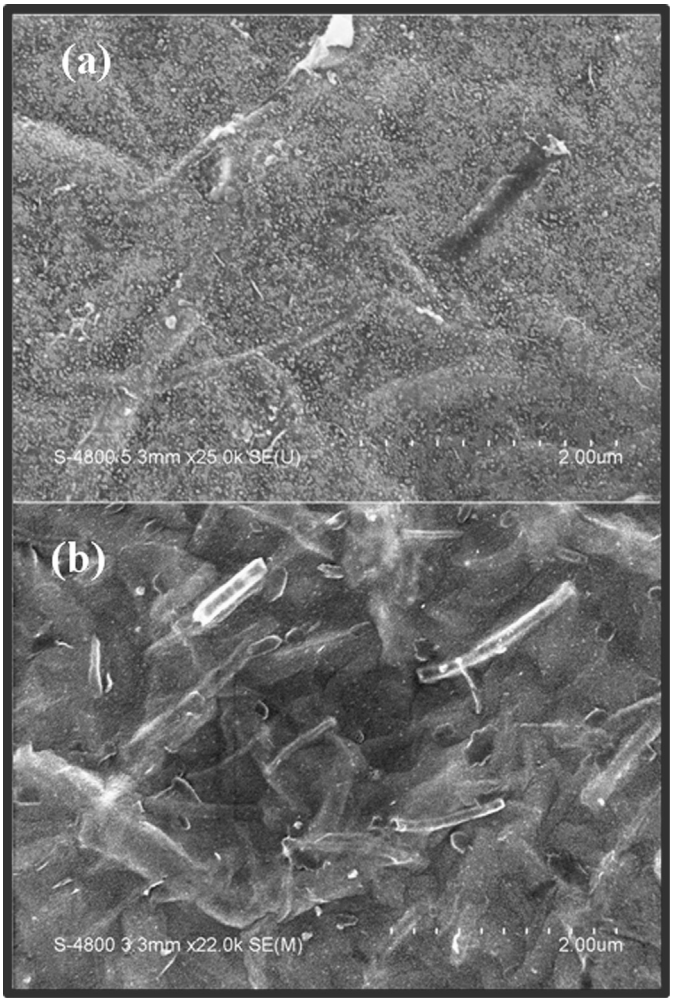

Fig. 6. SEM images of the CNT–GN papers after tests: (a) the 6.5CNT–20GN paper; (b) the 20CNT–10GN paper.

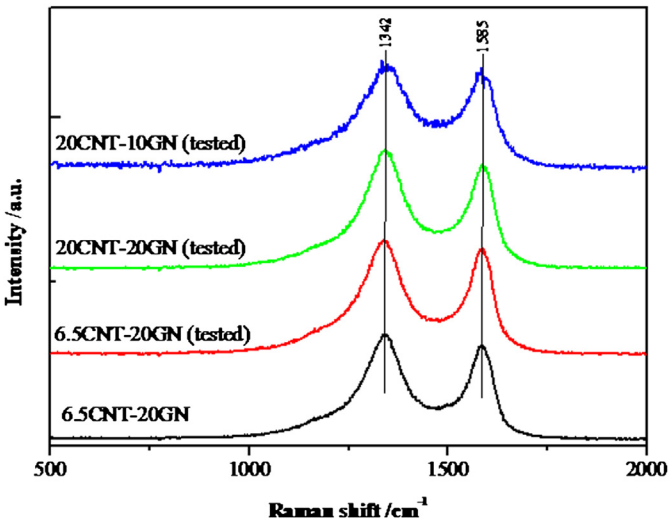

Fig. 7. Raman spectra of the CNT–GN papers after test.

of tested graphene papers [34]. Obviously, this results from GNS–electrolyte interactions. In contrast, the 20CNT–10GN surface is mainly covered with CNTs and the particles become even smaller. Accordingly, it can be suggested that during the process of lithium intercalation and decalation, the paper surface has broken down and more CNTs are accessible to Li ions.

Raman spectra of the tested papers are shown in Fig. 7. As compared to the untested 6.5CNT–20GN spectrum, no evident changes are observed in the spectra of the tested 6.5CNT–20GN and 20CNT–20GN paper. For the tested 20CNT–10GN spectrum, the intensity of the D-band is enhanced and is slightly over that of the G-band, indicating that more defect sites are created during battery performance. This is consistent with the SEM images in Fig. 6, i.e., the paper surface has broken down.

Following all these characterizations, the intrinsic factors that make major contribution to the improved battery performances of the CNT–GN hybrid papers can be approached. Powder based graphene, as a result of its open structure and hence high surface area, exhibits higher capacities than graphite does, offering reversible specific capacities higher than 400 mAh g^{-1} [3,4]. However, this unique feature is lost when the GNS are assembled into graphene paper, in which they are closely stacked. Thus, access of electrolyte to ALL the GNS is restrained and consequently, a barrier for Li diffusion into the GNS is established, leading to lower specific capacities of graphene papers. This situation holds for the CNT–GN hybrid paper when CNT content is relatively lower. In such hybrid papers, the CNTs are wrapped with GNS and hence, are hard to be accessible to Li and are of little contribution to Li storage. On the other hand, at higher CNT content, the CNTs are distributed throughout the GNS, effectively preventing restacking of the GNS. This allows more effective contact between the GNS and the electrolyte. Such an "open structure" of the hybrid papers, in turn, also enables more effective CNT–electrolyte contact, allowing Li to be stored in the CNTs. Notice CNTs are also a potential anode material for LIBs. These two facts explain the improved capacities of the hybrid papers.

Finally, for being complete, it is worth noting that the capacities can be even higher when more CNTs are introduced. However, this inevitably diminishes the mechanical strength of the hybrid paper, a situation that is not our primary purpose and we tried to avoid in this study. Nevertheless, a recent study proved that chemical functionalization of graphene will help maintain the mechanical strength of the graphene–CNT papers. Su et al., developed a novel approach toward highly conductive free-standing graphene/CNT composite films via an in situ thermolysis of functionalized graphene/organic cobalt complexes [35]. By combining 1D-CNT and 2D-graphene, a synergistic effect can be established for the hybrid materials. They also anticipated their potential applications in energy storage devices.

4. Conclusion

Graphene–carbon nanotube hybrid papers can be fabricated by the vacuum-assisted filtration of a mixture of GNS and CNTs suspended in water. The hybrid papers possess mechanical strength and flexibility that are comparable to those of graphene papers. Battery performances of these papers are highly dependent on the CNT/GN ratios. Highest performances are obtained in the 20CNT–10GN paper, which exhibits reversible capacities >330 mAh g^{-1} in the first 100 cycles at a current rate of 100 mA g^{-1}. In contrast, the capacities of the graphene paper of equal mass are only ~250 mAh g^{-1}. The presence of the CNTs plays a key role in the electrochemical performances of the hybrid papers. They effectively prevent restacking of the GNS, increase cross-plane electric conductivity of the paper and store Li. The graphene–CNT hybrid paper has a high potential to be used as collector and binder free anode for lithium ion batteries.

Acknowledgments

This research was supported by the Natural Science and Engineering Research Council of Canada (NSERC), Canada Research Chair (CRC) Program, Canadian Foundation for Innovation (CFI), Ontario Research Fund (ORF), Early Researcher Award (ERA) and the University of Western Ontario.

Appendix A. Supporting information

Supporting information related to this article can be found at http://dx.doi.org/10.1016/j.jpowsour.2013.02.065.

References

[1] Y. Wu, E. Rahm, R. Holze, J. Power Sourc. 114 (2003) 228–236.
[2] S. Flandrois, B. Simon, Carbon 37 (1999) 165–180.
[3] P. Lian, X. Zhu, S. Liang, Z. Li, W. Yang, H. Wang, Electrochim. Acta 55 (2010) 3909–3914.
[4] S. Yang, X. Feng, L. Wang, K. Tang, J. Maier, K. Mullen, Angew. Chem. Int. Ed. 49 (2010) 4795–4799.
[5] S. Yin, Y. Zhang, J. Kong, C. Zou, C. Li, X. Lu, ACS Nano 5 (2011) 3831–3838.
[6] H. Wang, L. Cui, Y. Yang, H. Casalongue, J. Robinson, Y. Liang, J. Am. Chem. Soc. 132 (2010) 13978–13980.
[7] G. Zhou, D. Wang, F. Li, L. Zhang, N. Li, Z. Wu, Chem. Mater. 22 (2010) 5306–5313.
[8] E. Yoo, J. Kim, E. Hosono, H. Zhou, T. Kudo, I. Honma, Nano Lett. 8 (2008) 2277–2282.
[9] D. Dikin, S. Stankovich, E. Zimney, R. Piner, G. Dommett, G. Evemeneko, Nature 448 (2007) 457–460.
[10] C. Wang, D. Li, C. Too, G. Wallace, Chem. Mater. 21 (2009) 2604–2606.
[11] H. Gwon, H. Kim, K. Lee, D. Seo, Y. Park, Y. Lee, Energy Environ. Sci. 4 (2011) 1277–1283.
[12] A. Abouimrane, O. Compton, K. Amine, S. Nguyen, J. Phys. Chem. C 114 (2010) 12800–12804.
[13] F. Liu, S. Song, D. Xue, H. Zhang, Adv. Mater. 24 (2012) 1089–1094.
[14] X. Zhao, C. Hayner, M. Kung, H. Kung, ACS Nano 5 (2011) 8739–8749.
[15] S. Li, Y. Luo, W. Lv, W. Yu, S. Wu, P. Hou, Adv. Energy Mater. 1 (2011) 486–490.
[16] J. Lee, K. Smith, C. Hayner, H. Kung, Chem. Commun. 46 (2010) 2025–2027.
[17] A. Yu, H. Park, A. Davies, D. Higgins, Z. Chen, X. Xiao, J. Phys. Chem. Lett. 2 (2011) 1855–1860.
[18] T. Kumar, R. Ramesh, Y. Lin, G. Fey, Electrochem. Commun. 6 (2004) 520–525.
[19] S. Ng, J. Wang, Z. Guo, G. Wang, H. Liu, Electrochim. Acta 51 (2005) 23–28.
[20] M. Park, S. Needham, G. Wang, Y. Kang, J. Park, S. Dou, Chem. Mater. 19 (2007) 2406–2410.
[21] B. Landi, M. Ganter, C. Cress, R. DiLeo, R. Raffaelle, Energy Environ. Sci. 2 (2009) 638–654.
[22] L. Cui, L. Hu, J. Choi, Y. Cui, ACS Nano 4 (2010) 3671–3678.
[23] S. Chen, P. Chen, Y. Wang, Nanoscale 3 (2011) 4323–4329.
[24] I. Lahiri, S. Oh, J. Hwang, S. Cho, Y. Sun, R. Banerjee, ACS Nano 4 (2010) 3440–3446.
[25] G. Wang, J. Yao, H. Liu, S. Dou, J. Ahn, Met. Mater. Int. 12 (2006) 413–416.
[26] S. Chou, Y. Zhao, J. Wang, Z. Chen, H. Liu, S. Dou, J. Phys. Chem. C 114 (2010) 15862–15867.
[27] S. Chen, W. Yeoh, Q. Liu, G. Wang, Carbon 50 (2012) 4557–4565.
[28] B. Vinayan, R. Nagar, V. Raman, N. Rajalakshmi, K. Dhathathreyan, S. Ramaprabhu, J. Mater. Chem. 22 (2012) 9949–9956.
[29] W. Hummers, R. Offeman, J. Am. Chem. Soc. 80 (1958) 1339.
[30] S. Suzuki, H. Hibino, Carbon 49 (2011) 2264–2272.
[31] M. Kalbac, Y. Hsieh, H. Farhat, L. Kavan, M. Hofmann, J. Kong, Nano Lett. 10 (2010) 4619–4626.
[32] X. Li, D. Geng, Y. Zhang, X. Meng, R. Li, X. Sun, Electrochem. Commun. 13 (2011) 822–825.
[33] M. Levi, D. Aurbach, J. Electrochem. Soc. 421 (1997) 79–88.
[34] Y. Hu, X. Li, D. Geng, R. Li, M. Cai, X. Sun, Electrochem. Acta 91 (2013) 227–233.
[35] Q. Su, Y. Liang, X. Feng, K. Mullen, Chem. Commun. 46 (2010) 8279–8281.